ESTIMATION OF FLUTTER BOUNDARIES IN THE PRESENCE OF STRUCTURAL UNCERTAINTY BY PROBABILISTIC AND FUZZY METHODS

Haddad Khodaparast, H., Marques, S., Badcock, K.J., Mottershead, J.E

Department of Engineering, University of Liverpool,
Harrison-Hughes Building, The Quadrangle, Liverpool L69 3GH
H.Haddad-Khodaparast@liverpool.ac.uk

SUMMARY: The problem of linear flutter analysis in the presence of structural uncertainty is addressed. Firstly the sensitivity of the transient decay rate coefficient/damping ratio with respect to a large number of uncertain structural parameters is evaluated close to flutter speeds in the aeroelastic model of a heavy rectangular (Goland) wing and a transport wing. Aeroelastic sensitivity analysis enables us to select effective random parameters in the both wing models. Secondly, interval, fuzzy and perturbation methods are used to propagate the structural uncertainty through the aeroelastic analysis resulting in regions of flutter-boundary uncertainty characterised by intervals, fuzzy membership functions and probability density functions. Monte Carlo Simulation is also used for verification purposes. First-order perturbation is generally found to produce results in good agreement with MCS, although there are differences at the tails of the distributions, especially for the unstable modes close to the flutter speed. Second-order perturbation provides an improved prediction of the nonlinear behaviour at the tails. The flutter membership function predicted by the fuzzy method generally encloses the tails of the MCS distribution but is perhaps too generous, leading to over-prediction of uncertainty intervals at the flutter boundary. Variability in structural mass and stiffness parameters is shown to have a significant affect upon the flutter intervals. Structural damping results in a small but significant increase in the flutter speed, but structural-damping variability does not translate into significant intervals of flutter-boundary uncertainty. Studies are carried out on the Goland wing, with and without structural damping, and on a transport wing model.

KEYWORDS: Interval flutter analysis, Fuzzy method, perturbation method, linear flutter analysis.

1. Introduction

The accurate estimation of flutter boundaries is an important problem in aircraft certification. When the structural model includes parameter uncertainties, represented by intervals, fuzzy membership functions or probability density functions, then this uncertainty may be propagated through the aeroelastic model resulting in uncertain flutter boundaries, described correspondingly in terms of intervals, fuzzy memberships and probability densities. The review paper by Pettit [1] and references therein show the considerable attention that has already been paid to this subject. This paper is specifically concerned with aeroelastic analysis in the presence of structural uncertainty, and the evaluation of various propagation methods.

Variability in structural parameters arising from the accumulation of manufacturing tolerances or environmental erosion is considered in this paper. Structural variability must be characterised and the first step in achieving this is to discover which of the uncertain structural parameters have a significant affect on the aeroelastic analysis. The distribution or range of these parameters must be estimated. This variability may then be propagated through the model to determine a distribution or range of flutter speeds. In a small number of research papers [1] flutter-speed estimates are determined in the presence of parameter uncertainty. Kurdi et al. [2] used MCS to propagate the variation in dimensional properties of the structural parameters of the Goland wing in order to quantify the flutter-speed probability density function. Results showed the flutter speed to be highly sensitive to small changes in the structure. Attar and Dowell [3] used a response surface method to identify the effect of uncertainty on the response of a nonlinear aeroelastic system. Results were found to be in good agreement with those obtained by MCS. More recently, Verhoosel et al. [4] used stochastic finite element models to perform

uncertainty and reliability analysis on fluid-structure stability boundaries. They found the sensitivity-based methods capable of characterising the statistical moments of the aeroelastic response.

In this paper a sensitivity study is carried out to select uncertain structural parameters. Then three different approaches are considered for the characterisation of flutter-speed uncertainty. In the first approach, an interval flutter analysis is used. This method is said to be 'possibilistic' since no assumption is made about the probability distribution of either the structural parameters or the flutter speeds. Consequently the interval flutter method is restricted to the evaluation of upper and lower bounds without providing any information on how the uncertainty is distributed within such bounds. The interval flutter analysis requires a minimisation and a maximization of the damping ratios at each velocity. The second approach makes use of fuzzy logic so that the uncertainty is defined according to a membership function. The fuzzy finite element method has been used recently by Moens and Vandepitte [5] for the calculation of uncertain frequency response functions of damped structures. The fuzzy method is implemented within a number of α-levels for the numerical solution of the interval finite element problem at each level. The third procedure is a probabilistic perturbation approach that makes use of the theory of quadratic forms [6]. Each solution of the flutter equation is perturbed about the mean values of the uncertain parameters through a truncated Taylor series expansion. Then the statistical moments of the damping ratio at the unstable mode are calculated. The procedure requires the calculation of the sensitivity and Hessian matrices. Finally the three propagation methods are applied to the Goland wing [2] and to a model of a transport wing. It is found in these examples that variability in structural damping has less effect on flutter speed intervals than does variability in structural mass and stiffness. Results achieved by first-order perturbation are found to be in good agreement with those obtained from MCS for the damping ratios not contributing to the flutter. However there are differences at the tails of the distributions for the flutter modes, close to the flutter speed. The nonlinearity at the tails of the probability density functions can be estimated by both second-order perturbation and fuzzy methods. More details of the methods and results of this study can be found in [7].

1. PROPAGATION METHODS

1.1. Interval and Fuzzy method

Flutter and flutter sensitivity analysis were carried out using the aerodynamic module of MSC-NASTRAN, using the double-lattice subsonic lifting surface theory (DLM), described by Katz and Plotkin [8]. The flutter analysis is described as a nonlinear eigenvalue problem and ttherefore it is necessary to apply global optimisation procedures in search of the maximum and minimum values of damping ratio that define the extent of an interval of flutter uncertainty. The optimisation problem may be expressed by the following statement.

Determine,

$$\left\lfloor \underline{\gamma}_i, \overline{\gamma}_i \right\rfloor = \left[\min\left(\gamma_i\right), \max\left(\gamma_i\right) \right] \tag{1}$$

subject to,

$$\left[\mathbf{A}\left(\boldsymbol{\theta}, \omega_i\right) - \lambda_i \mathbf{I}\right]\left(\mathbf{u}_i\right) = \mathbf{0}; \quad \underline{\boldsymbol{\theta}} \le \boldsymbol{\theta} \le \overline{\boldsymbol{\theta}} \tag{2}$$

where,

$$\mathbf{A} = \begin{bmatrix} \mathbf{0} & \mathbf{I} \\ -\mathbf{M}^{-1}\left[-\frac{1}{2}\rho V^2 \mathbf{E} + \mathbf{K}\right] & -\mathbf{M}^{-1}\left[-\frac{1}{4}\rho \bar{c} V \mathbf{B}/k + \mathbf{C}\right] \end{bmatrix} \tag{3}$$

$\mathbf{M}$, $\mathbf{B}$, $\mathbf{E}$, $\mathbf{C}$ and $\mathbf{K}$ are respectively the mass, aerodynamic damping, aerodynamic stiffness, structural damping and structural stiffness. Also V is the airspeed, ρ is the air density, $\bar{c}$ is aerodynamic aerofoil chord, $k = \bar{c}\,\omega_i / 2V$ is reduced frequency (a function of circular frequency f_i, $\omega_i = 2\pi f_i$), $\underline{\bullet}$ and $\overline{\bullet}$ represent the lower and upper bounds of $\bullet$ respectively, γ_i is damping ratio which appears in the real part of the eigenvalue $\lambda_i = \omega_i\left(\gamma_i \pm i\right)$ and $\boldsymbol{\theta} \in \Re^{m\times 1}$ is the vector of uncertain system parameters. Once upper and lower bounds,

$\bar{\gamma}_i$, $\underline{\gamma}_i$, of the damping ratios are found it is possible to extract the upper and lower bounds of the flutter speed by curve fitting to discrete points in the region of the flutter speed as shown in Figure 1(a).

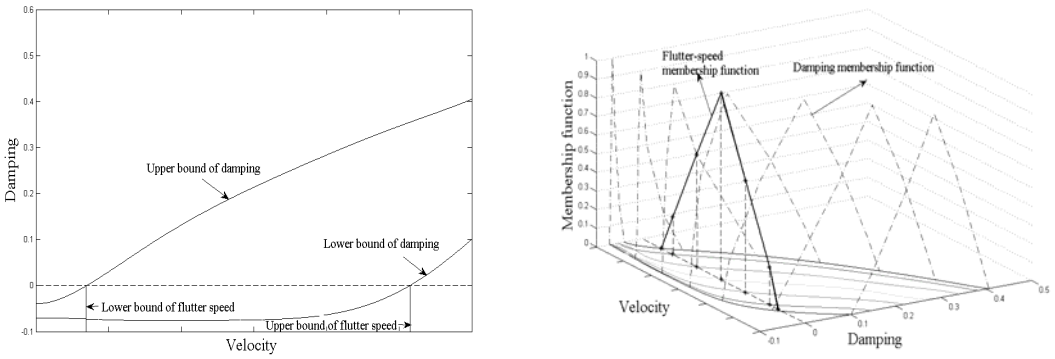

Figure 1 – (a) Extracting flutter speeds bounds from bounds on the damping ratios of the flutter mode, (b) Extracting the flutter-speed membership function from the damping membership functions at selected velocities.

The fuzzy finite element method involves the application of a numerical procedure at a number of α-levels as explained in [5]. In our particular application the fuzzy-output membership function is the damping ratio of a flutter eigenvalue. The method is described in detail in [5]. Application of the fuzzy propagation method at velocity increments close to the deterministic flutter speed results in the construction of damping membership functions, denoted as damping membership functions in Figure 1(b). The intersection of the damping membership functions with the zero-damping plane results in a number of discrete points, which when connected by straight lines define the flutter-speed membership function. This latter membership function is shown with solid line in Figure 1(b).

1.2. Perturbation method using the theory of quadratic forms

The damping ratio at a fixed speed V can be expanded about the mean value of the uncertain parameters as,

$$\gamma_i = \gamma_i(\bar{\boldsymbol{\theta}}) + \sum_{j=1}^{m} \left.\frac{\partial \gamma_i}{\partial \theta_j}\right|_{\theta_j=\bar{\theta}_j} \left(\theta_i - \bar{\theta}_i\right) + \sum_{j=1}^{m}\sum_{k=1}^{m} \left.\frac{\partial^2 \gamma_i}{\partial \theta_j \partial \theta_k}\right|_{\substack{\theta_j=\bar{\theta}_j \\ \theta_k=\bar{\theta}_k}} \left(\theta_j - \bar{\theta}_j\right)\left(\theta_k - \bar{\theta}_k\right) + \ldots \tag{4}$$

Statistical moments of the damping ratios can be determined using the theory of quadratic forms [6]. Then the probability density function may be evaluated using Pearson's theory [9] as,

$$\frac{dp(\gamma_i)}{d\gamma_i} = \frac{a+\gamma_i}{b_0 + b_1\gamma_i + b_2\gamma_i^2}\, p(\gamma_i) \;\Rightarrow\; p(\gamma_i) = \exp\left(\int \frac{a+\gamma_i}{b_0 + b_1\gamma_i + b_2\gamma_i^2}\, d\gamma_i\right) \tag{5}$$

The details of above analysis can be found in [7].

As mentioned earlier, Monte Carlo Simulation is also used for verification purposes. Whichever propagation method (interval, fuzzy or probabilistic) is used, an issue of very practical significance is the initial estimation of the parameter uncertainty to be propagated. In this paper we address only the uncertainty associated with the structural model. One approach to this problem is to apply stochastic model updating, as described for example by the present authors [11].

2. NUMERICAL EXAMPLES

2.1. The Goland wing without structural damping

The finite element model of the heavy version of the Goland wing is considered. Full details of the wing geometry, the finite element model and aerodynamic models are provided in reference [4]. The wing is

composed of upper and lower skins, three spars, eleven ribs, three spar caps, eleven rib caps and 33 posts (1-D elements) with nominal, but uncertain, thicknesses and areas as defined in [7]. The sensitivities of damping ratios with respect to the normalised structural parameters were evaluated at four velocities close to the flutter speed at different Mach numbers. Solving the deterministic flutter equation at the mean values of the random parameters showed that flutter occurred in the first mode for the complete range of Mach numbers chosen. The sensitivities, scaled to avoid ordering effects, were found to be greater for the lower Mach numbers than the higher ones. From the values of the sensitivities for the Mach number of 0.7, it was seen that among the 63 random parameters, just seven (the thicknesses of upper and lower wing skins, thicknesses of trailing and leading edge spars and the areas of leading, trailing and center cap) were capable of significantly changing the damping ratio and the flutter speed. The damping ratios were found to be most sensitive to same seven parameters at different Mach numbers. For interval analysis, the selected random parameters were considered to be in intervals defined by $\pm 5\%$ of the mean values. The damping ratios and frequencies of modes 1 and 2 are shown in Figures 2(a) and 2(b). MCS was used to verify the results obtained by interval analysis using samples generated from uniform distributions. It can be seen from Figure 2, that a good agreement between results obtained from interval analysis and MCS is achieved. Also from Figure 2(a) it is observed that the flutter speed is defined within the interval from 410 ft/s to 440 ft/s at Mach 0.7. It was observed that modes 3 and 4 remain stable at all the velocities considered. The flutter-speed bounds versus Mach numbers are shown in Figure 3 where it is seen that the interval-analysis and MCS results are in good agreement.

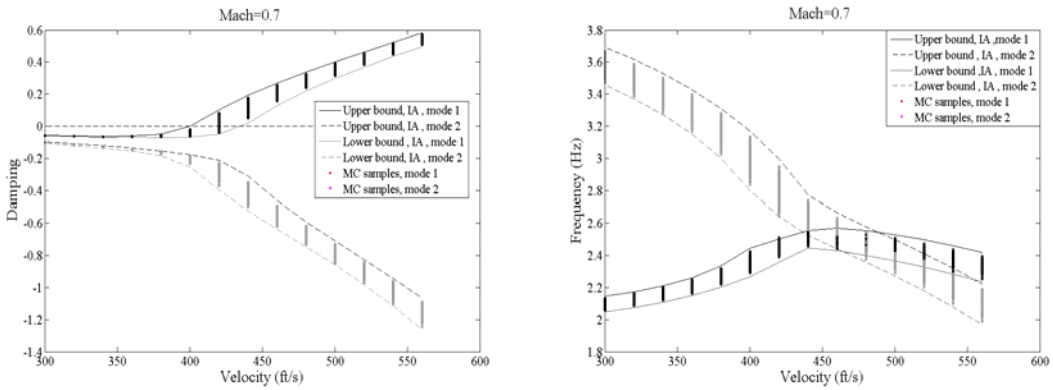

Figure 2 – Interval and MCS results for (a) damping ratios and (b) frequencies of modes 1 and 2.

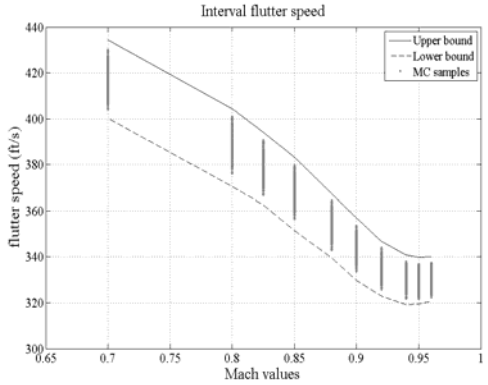

Figure 3 – Interval and MCS results showing flutter speeds versus Mach values.

Gaussian distributions were chosen for the probability perturbation analysis using seven randomised parameters with coefficients of variation $\mathrm{COV} = 0.05$. Other parameters were taken to be deterministic. Propagation methods were applied to the Goland wing to estimate the output pdfs. In MCS, 1000 samples were taken from the parameter pdfs. For propagation by the fuzzy method, the Gaussian probability density functions of system parameters were approximated by triangular membership functions as explained in [12]. As mentioned previously, application of the fuzzy propagation method at velocity increments close to the deterministic flutter speed results in the construction of damping ratio membership functions.

The increments used in approximating the sensitivities by using forward differences should be chosen carefully. The bounds of the damping ratios at different velocities by first order perturbation using gradients calculated by MSC-NASTRAN and by finite difference approximation were compared. Apart from the velocity of 420ft/s, very close to the threshold of instability, excellent agreement between the two sets of results was found.

Figures 4 (a) and (b) show the perturbation and MCS results for the damping ratios and frequencies of the first two modes, with the mean MCS result given by the solid lines. The bounds of the damping ratios and frequencies obtained from first-order and second-order perturbation methods are also shown. It is seen from Figure 4 that whereas the variability of the frequencies remains unchanged throughout the velocity range, the damping ratios become more sensitive as the flutter speed is approached and at higher velocities the damping ratio variability becomes similar in extent to the frequency variability. This result demonstrates how the aeroelastic damping ratio becomes dependent upon the mass and stiffness structural parameters at the flutter speed and beyond. At low speeds the damping ratios are mostly unaffected by M and K variability so that in this range the behaviour is similar to normal-mode structural behaviour. Scatter diagrams in Figures 5 (a) and (b) show the variability in the aeroelastic damping ratios and frequencies at 300 ft/s (below the flutter speed). An ellipse at two standard deviations is superimposed upon the scatter in Figure 5(b). The aeroelastic damping ratio variability is limited to a small condensed area in the real-part eigenvalue space, whereas the aeroelastic frequency variability appears as a random scattering of points over a wider frequency range in the space of the imaginary parts of the eigenvalues. Figures 6 (a) and (b) show the scatter of the damping ratios and frequencies at 420 ft/s, where it is seen that the scatter diagram for the damping ratio has a particular structure close to a 45° line. We observe that if a scatter point is chosen that corresponds to reduced damping ratio in aeroelastic mode 1 then the damping ratio in mode 2 is increased to a similar degree and vice-versa. We know that the aeroelastic eigenvalues can be expressed as a complex linear combination of the structural normal-mode eigenvalues. Therefore, we can write the first and second complex aeroelastic eigenvalues approximately as $\lambda_1(\boldsymbol{\theta}) \approx \alpha_1 \lambda_1^{(n)}(\boldsymbol{\theta}) + \alpha_2 \lambda_2^{(n)}(\boldsymbol{\theta})$ and $\lambda_2(\boldsymbol{\theta}) \approx \beta_1 \lambda_1^{(n)}(\boldsymbol{\theta}) + \beta_2 \lambda_2^{(n)}(\boldsymbol{\theta})$ where $\alpha_1, \alpha_2, \beta_1, \beta_2$ are complex functions of velocity and the superscript (n) distinguishes a real structural normal-mode eigenvalue from an aeroelastic eigenvalue. At low velocities $\alpha_2, \beta_1 \to 0, \alpha_1, \beta_2 \to 1$ so that the aeroelastic eigenvalues are close to the normal-mode eigenvalues. At higher speeds the complex constants are given more generally by $0 \le |\alpha_1|, |\alpha_2|, |\beta_1|, |\beta_2| \le 1$ so that the damping ratios of the aeroelastic eigenvalues include structural mass- and stiffness-variability present in the normal mode eigenvalues. It appears that at the flutter boundary the uncertainty in the aeroelastic damping ratio has a particular structure that renders the unstable mode less damped while the stable mode is rendered more damped, and vice versa. It is clear from Figure 4(a) that the first aeroelastic mode becomes unstable.

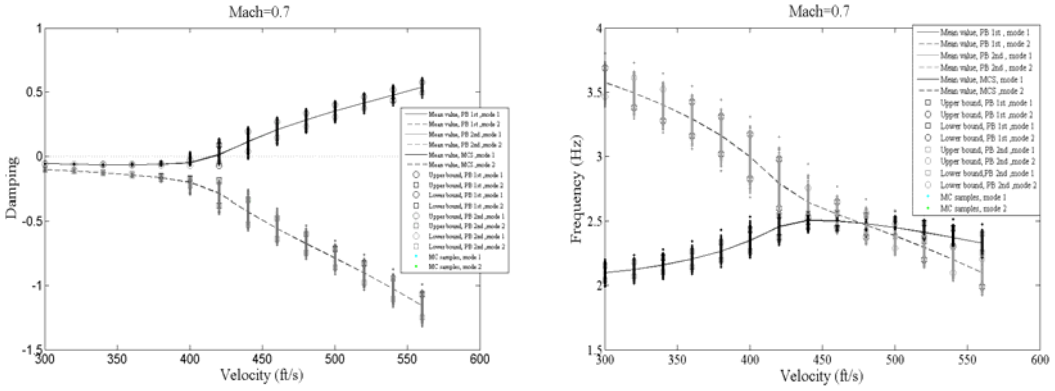

Figure 4 – Perturbation and MCS results, (a) damping ratios of modes 1 and 2, (b): imaginary parts of modes 1 and 2.

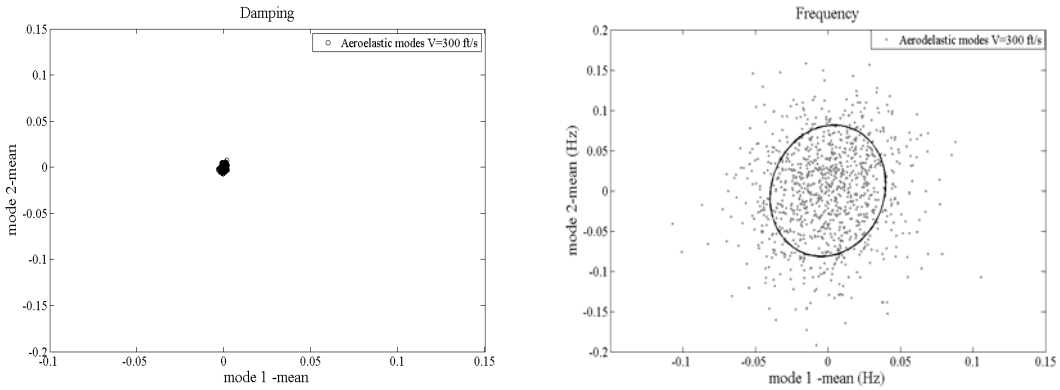

Figure 5 – Scatter of the aeroelastic eigenvalues at 300 ft/s (a) real-part, (b) imaginary part.

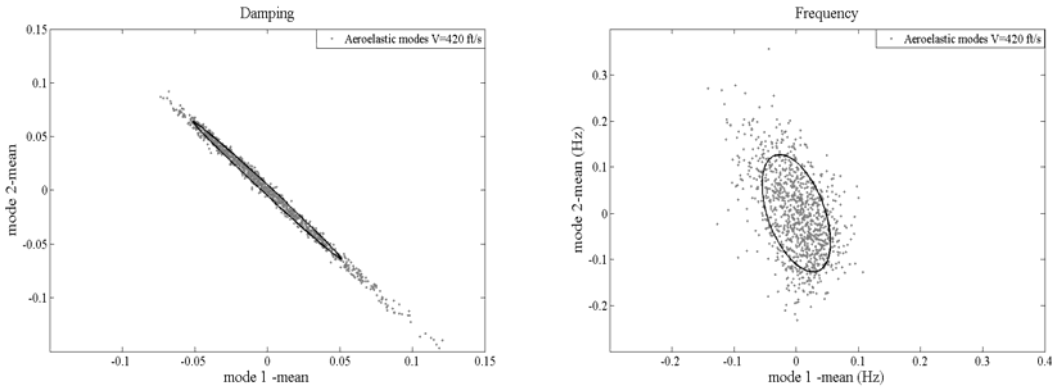

Figure 6 – Scatter of the aeroelastic eigenvalues at 420 ft/s (a) real-part, (b) frequency.

The first-mode damping ratio distributions by first- and second-order probabilistic perturbation, fuzzy methods, and MCS are shown together in Figure 7(a) at velocity 420 ft/s. Although the first-order perturbation accurately captures most of the pdf generated by MCS, it is clear that there are differences at the tails that might be important from a practical engineering point of view. The tails are better represented by the second-order perturbation, which is close to the MCS result at the tails but does not match the mean value obtained by MCS. Possibly this discrepancy is due to the approximation of the Hessian matrix by forward differences. The fuzzy membership function extends beyond the tail of the damping ratio distribution on the positive side and therefore offers a conservative estimate of the flutter boundary (when combined with membership functions at other velocities as in Figure 1(b)). Mean values of the damping ratios are shown in Figure 7(b) together with MCS results at 420 ft/s.

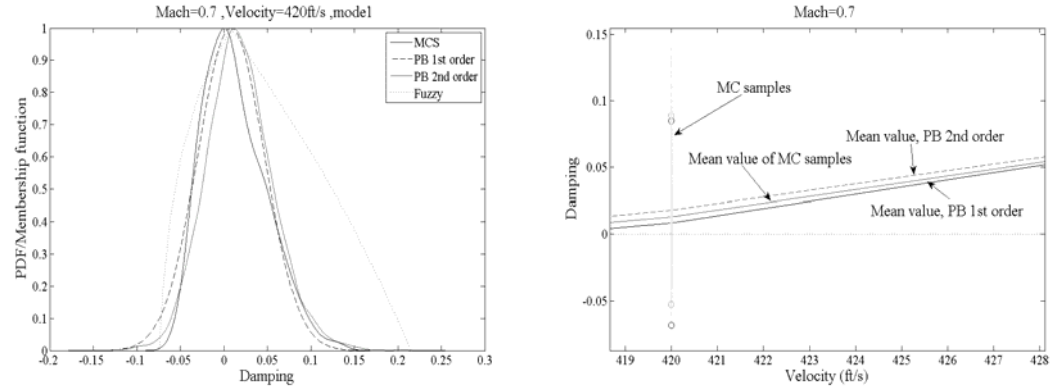

Figure 7 – Velocity 420ft/s: (a) pdf and membership function, (b) MCS, mean value of MCS and mean values obtained by 1st and 2nd order perturbation.

Figure 8(a) shows the flutter-speed distributions obtained by probabilistic perturbation, fuzzy methods and MCS. In Figure 8(b) it is seen that the fuzzy method consistently over-estimates the flutter boundary at different Mach numbers, whereas the perturbation result consistently underestimates it.

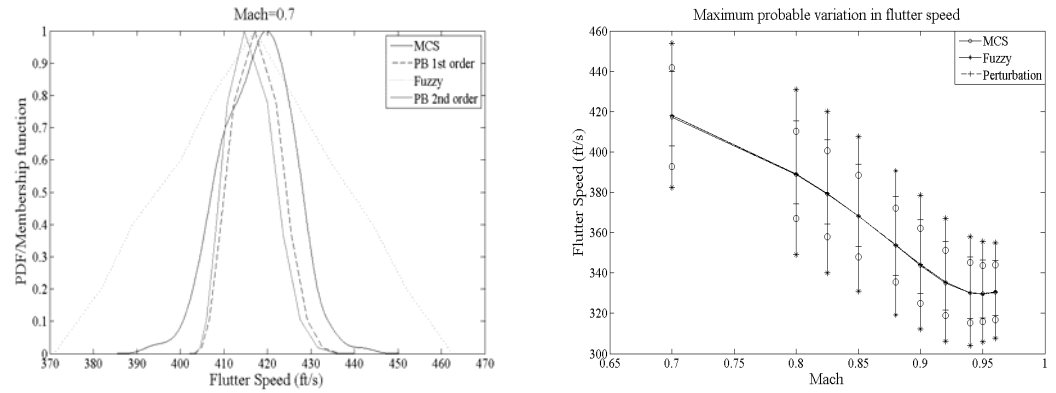

Figure 8 – (a) Flutter speed pdf and membership function, (b): flutter speed.

2.2. The Goland wing with structural damping

The effect of structural damping on the flutter stability boundaries was considered by adding twelve dashpot elements, uniformly located along the length of the Goland wing from tip to root. Complex eigenvalue analysis was carried out, resulting in modal damping parameters for the first four modes, 3.403772×10^{-2}, 1.345800×10^{-2}, 4.506277×10^{-2} and 4.539254×10^{-2}, being representative of structural damping in an aircraft wing. A small but significant increase in the flutter speed was observed when structural damping was included. Then Gaussian distributions were chosen for the twelve damping parameters with mean values of 200 lb.s/ft and coefficients of variation COV = 0.05 . Probabilistic perturbation and MCS was found to result in very narrow bands of variation for the damping ratios and frequencies.

The results obtained by different methods from numerous test cases, with and without structural damping, show that reliable flutter boundary estimates may be obtained by interval analysis. Therefore it was decided to use interval analysis for the test case described in the following section.

2.3. Transport wing with uncertainty in connection of wing-to-Fuselage

The FE model of a commercial transport wing, with a span of 36 meters, is considered. This model is an example of a large modern transport aircraft [13, 14]. Full details of structural and aerodynamic models are given in [13, 14]. A clamped version of the wing was studied in [13, 14]. Because the clamped model is not realistic, we changed the boundary conditions of the FE model to elastic support. This has been done by adding spring elements at roots. Coefficients of spring elements were defined in intervals of $[1\times10^{7}\ 1\times10^{10}]$ N/m. As shown in Figure 11, solving the deterministic flutter equation at the mean values of the uncertain parameters showed that flutter occurred in the third mode for the Mach number 0.85. As it can be seen from Figure 11 the deterministic flutter speed was found to be 325m/s. Figure 11 shows the interval analysis results for the third-mode damping ratio close to the flutter speed. The minimum and maximum bound of flutter speed were found to be 315 m/s and 340 m/s respectively.

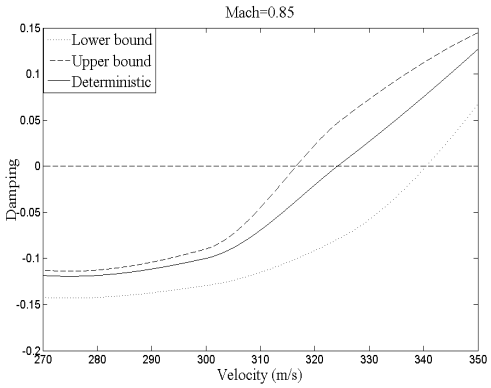

Figure 9 – The third-mode damping ratio bounds close to the flutter speed by interval analysis.

3. CONCLUSION

Different forward propagation methods, interval, fuzzy and perturbation, were applied to linear aeroelastic analysis for a variety of wing models. Sensitivity analysis was used to select parameters for randomisation that had a significant effect on flutter speed. These random parameters were then propagated through the aeroelastic analysis to obtain estimates of intervals, fuzzy membership functions or pdfs for the damping ratio and flutter speed. Interval analysis was found not only to be computationally efficient but also to provide a sufficiently good approximation to flutter bounds determined by MCS. Nonlinear behaviour was observed in the tails of the damping ratio pdfs of the flutter mode. Second-order probabilistic perturbation analysis was found to represent the behaviour at the tails with acceptable accuracy, whereas the fuzzy approach led to conservative solutions. Flutter analysis of the Goland wing showed the instability to be critically dependent upon certain structural mass and stiffness terms. At velocities less than the flutter speed, the intervals of uncertainty on aeroelastic damping were found to be small, but increased at around the flutter speed and beyond to become similar in extent to the bounds on the frequencies across the entire range of frequencies. Structural damping variability had virtually no effect upon the intervals of the aeroelastic damping ratios and therefore upon the flutter intervals. At velocities close to the flutter speed a particular structure was revealed, close to a 45° line, in the scatter diagrams of the damping ratios. Then for a chosen point where the unstable mode was rendered less damped, the stable mode

became more damped to a similar degree, and vice-versa. Interval flutter analysis is also carried out in a commercial transport wing with uncertain boundary conditions. Flutter bounds were determined by the propagation of structural stiffness parameters by interval analysis.

ACKNOWLEDGEMENTS

This research is funded by the European Union for the Marie Curie Excellence Team ECERTA under contract number MEXT-CT-2006-042383.

4. REFERENCES

[1] Pettit, C. Uncertainty Quantification in Aeroelasticity: Recent Results and Research Challenges. Journal of Aircraft. 41 (5), 2004,1217–1229.

[2] Kurdi, M., Lindsley, N. and Beran, P., Uncertainty quantification of the Goland wing's flutter boundary, AIAA Paper 2007-6309, August 20-22.

[3] Attar, P.J., Dowell, E.H, Stochastic analysis of a nonlinear aeroelastic model
using the response surface method. Journal of Aircraft. Vol. 43, No. 4, July–August 2006, 43 (4), 2006, 1044–1052.

[4] Verhoosel C.V., Scholcz T.P., Hulshoff S.J., Gutiérrez M.A. , Uncertainty and Reliability Analysis of Fluid–Structure Stability Boundaries, AIAA Journal 47 (1) (2009) 91–104.

[5] Moens, D. and Vandepitte, D., A fuzzy finite element procedure for the calculation of uncertain frequency response functions of damped structures: Part 1 – procedure. Journal of Sound and Vibration 2005; 288(3):431–62.

[6] Adhikari, S. and Friswell, M.I., Random matrix eigenvalue problems in structural dynamics. International Journal for Numerical Methods in Engineering, 69, 2007, 562-591.

[7] Haddad Khodaparast, H., Mottershead, J.E, Badcock, K.J., Propagation of Structural Uncertainty to Linear Aeroelastic Stability, Computers and Structures, submitted.

[8] Katz, J. and Plotkin, A., Low-Speed Aerodynamics, Cambridge University press, 2001.

[9] Pearson, K., Contributions to the mathematical theory of evolution, II: Skew variation in homogeneous material. Philosophical Transactions of the Royal Society of London ARRAY, 1895, 186: 343–414.

[10] Bowman, A.W., and Azzalini, A., Applied Smoothing Techniques for Data Analysis, Oxford University Press,1997.

[11] Khodaparast H.H., Mottershead J.E., Friswell M.I., Perturbation methods for the estimation of parameter variability in stochastic model updating, Mechanical Systems and Signal Processing, 22 (8) (2008) 1751–1773.

[12] Hanss, M. and Willner, K., A fuzzy arithmetical approach to the solution of finite element problems with uncertain parameters. Mechanics Research Communications, 27(3):257–272, 2000.

[13] Girodroux-Lavigne, P., Grisval, J. P., Guillemot, S., Henshaw, M., Karlsson, A., Selmin, V., Smith, J., Teupootahiti, E. and Winzell, B., Comparison of static and dynamic fluid-structure interaction solutions in the case of a highly flexible modern transport aircraft wing, Aerospace Science and Technology, 7, 2003, 121-133

[14] Taylor, N.V., Allen, C.B., A. L. Gaitonde , Jones, D.P, Vio, G.A., Cooper, J.E., Rampurawala A. M., Badcock, K.J., Woodgate, A.M., Henshaw, M. J. de C., A Comparison of Linear and Nonlinear Flutter Prediction Methods: A Summary of PUMA DARP Aeroelastic Results, Aeronautical Journal, 110 (1107), May, 2006,333-343.